Crystal precipitation and dissolution in a thin strip

CRYSTAL PRECIPITATION AND DISSOLUTION IN A THIN STRIP*

T.L. VAN NOORDEN†

Abstract. A two-dimensional micro-scale model for crystal dissolution and precipitation in a porous medium is presented. The local geometry of the pore is represented as a thin strip. The model allows for changes in the pore volume. A formal limiting argument leads to a system of 1D effective upscaled equations. The effective equations allow for travelling wave solutions. Existence and uniqueness of these travelling wave solutions are proven. Numerical solutions of the effective equations are compared with numerical solutions of the original equations on the thin strip and with analytical results. Also a comparison is made with a model from the literature that does not allow changes in the pore volume.

1. Introduction. In this paper we derive, using a formal limiting procedure with asymptotic expansions, a macroscopic law for crystal dissolution and precipitation in a porous medium. The microscopic model that serves as the starting point for the limiting process, incorporates the change in volume of the pore space as a result of the precipitation/dissolution process. We also study travelling wave solutions of the macroscopic law and the behaviour of solutions of the obtained macroscopic law is numerically compared to the behaviour of solutions of the corresponding microscopic model.

Macroscopic laws for reactive transport in porous media, which include the present case of crystal dissolution and precipitation, are of practical importance in many physical, biological and chemical applications. Macroscopic laws for reactive transport in porous media are derived rigorously in, e.g., [5]. For the more specific case of crystal dissolution and precipitation, macroscopic models are given in [3, 4, 6, 7]. In these papers the presented macroscopic models are analysed, but are not supported by a rigorous derivation. In most of these papers also the numerical solution of the proposed model equations is studied. Related work, in which the transport of dissolved material is analysed, can be found in [12, 14].

The main difficulty in performing the formal homogenization for the crystal dissolution and precipitation reaction is that the equations that describe the microscale processes contain a free boundary. This free boundary describes the interface between the layer of crystalline solid attached to the grains and the fluid occupying the pores. The location of this free boundary is an unknown in the model and moves with speed proportional to the local dissolution/precipitation rate. The microscale model with the free boundary has been studied in [15] in a one dimensional setting and without flow. Other works that study crystal dissolution and precipitation on the microscale are [8] and [9].

The crystal dissolution and precipitation problem has been studied also in [6] and [13, 16]. The main difference between the cited papers and the present paper is that in the cited papers it is assumed that the thickness of the layer of crystalline solid attached to the grains is negligible so that the pore geometry can assumed to be fixed. In this case the formal homogenization is a standard procedure and the macroscopic equations can be derived straightforwardly. (For completeness and for comparison reasons, we will

*Part of this research has been funded by the Dutch BSIK/BRICKS project.

†Department of Mathematics and Computer Science, Technische Universiteit Eindhoven, P.O. Box 513, 5600 MB Eindhoven, The Netherlands, email: T.L.v.Noorden@tue.nl

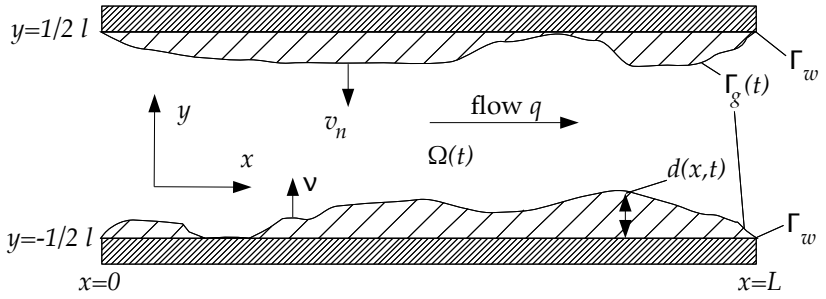

FIG. 2.1. *Schematic representation of a 2D thin strip with layers of crystalline solid attached to the strip boundary.*

shortly discuss the derivation of the macroscopic equations for the fixed geometry cases in Section 3.)

In this paper we do take into account the change in the pore volume due to the precipitation/dissolution reaction. For the microscale model this results in a free-boundary problem, and for the macroscopic model this results in a permeability and porosity that depend on the local pore geometry. The behaviour of solutions of the microscale model are numerically studied using the Arbitrary Lagrangian Eulerian method and also analytically by considering travelling wave solutions.

The structure of this paper is as follows. In Section 2 we will discuss the model equations that describe the processes in the thin strip. In Section 3, we will derive using a formal limiting argument the effective equations for the limit of the thickness of the strip to zero. Travelling wave solutions to the effective equations are studied in Section 4. In Section 5 the results obtained for the travelling wave solutions are compared to the results for the effective equations studied in [6, 11], and in Section 6 numerical results for both the microscale model and the effective equations are presented and compared.

2. Model equations. We consider the following model for crystal dissolution and precipitation in a pore. The pore space is represented by a two dimensional thin strip, of length L [m], and width l [m]. The two dimensional bounded domain Ω, representing the strip, is given by

$$\Omega := \{(x, y) \in \mathbb{R}^2 | 0 \leq x \leq L,\ -1/2l \leq y \leq 1/2l\},$$

A layer of crystalline solid may be attached to the boundaries of the strip, and we assume that the thickness of the layers on both upper and lower boundary are equal, so that the geometry is symmetric with respect to the x-axis. The thickness of this layer is given by $d(x, t)$ [m]. Let

$$\Omega(t) := \{(x, y) | 0 \leq x \leq L,\ -(1/2l - d(x, t)) \leq y \leq (1/2l - d(x, t))\}$$

denote the (variable) region occupied by a fluid in which cations (M_1) and anions (M_2) are dissolved. Here we assume that $d(x, t) < 1/2l$. The case $d = 1/2l$ corresponds to the situation that the strip is blocked by the crystalline solid, and we do not consider this situation in the present paper.

The boundary of $\Omega(t)$ can be split into 3 parts: the interface of the crystalline layer with the fluid, denoted by $\Gamma_g(t)$, which is defined by

$$\Gamma_g(t) := \{(x,y)|0 < x < L,\, y = \pm(1/2l - d(x,t))\},$$

the boundary at $x = 0$, denoted by $\Gamma_i(t)$:

$$\Gamma_i(t) := \{(x,y)|x = 0,\, -(1/2l - d(x,t)) \leq y \leq 1/2l - d(x,t)\},$$

and the boundary at $x = L$, denoted by $\Gamma_o(t)$:

$$\Gamma_o(t) := \{(x,y)|x = L,\, -(1/2l - d(x,t)) \leq y \leq 1/2l - d(x,t)\}.$$

In a precipitation reaction n_1 cations of M_1, and n_2 anions of M_2 can precipitate in the form of one molecule of a crystalline solid M_{12}, which is attached to the boundary. The reverse dissolution reaction is also possible. Let c_i $[\frac{\text{mol}}{\text{m}^2}]$ denote the molar concentration of M_i, with $i = 1, 2$, and let c_f denote the molar concentration of the fluid phase in which the anions and cations are disolved. Then c_i and c_f satisfy the convection-diffusion equations in $\Omega(t)$

$$\begin{aligned} \partial_t c_i &= \nabla \cdot (D_i \nabla c_i - q_i c_i), \quad \text{for } i = 1, 2, \\ \partial_t c_f &= \nabla \cdot (D_f \nabla c_f - q_f c_f), \end{aligned}$$

where D_i and D_f $[\frac{\text{m}^2}{\text{s}}]$ are the diffusion coefficients for the different dissolved ions and the fluid phase, respectively, and where q_i and q_f $[\frac{\text{m}}{\text{s}}]$ denote the velocities of the different components.

At this point we make the assumption that the sum of the molar concentrations of the cations, the anions and the fluid phase is constant, which may be justified by assuming that the concentration of ions in the fluid is small. This means that we have

$$c_f + c_1 + c_2 \equiv \rho_f, \tag{2.1}$$

where ρ_f $[\frac{\text{mol}}{\text{m}^2}]$ is a fixed molar concentration. From this assumption it follows that the diffusion coefficients and also the velocities for all the components are equal:

$$\begin{matrix} D := D_f = D_i \\ q := q_f = q_i \end{matrix} \quad \text{for } i = 1, 2.$$

At the interface of the layer attached to the boundary of the strip, we have by conservation of mass

$$\nu \cdot (D \nabla c_i - q c_i) = v_n(n_i \rho_c - c_i), \text{ on } \Gamma_g(t), \tag{2.2}$$

where ρ_c $[\frac{\text{mol}}{\text{m}^2}]$ denotes the molar density of the crystalline solid, and where ν denotes the outward pointing normal and is given by

$$\nu = (\partial_x d, -1)^T / \sqrt{1 + (\partial_x d)^2} \tag{2.3}$$

for the lower boundary, and where v_n $[\frac{\mathrm{m}}{\mathrm{s}}]$ denotes the normal velocity of the interface. The normal velocity of the interface is proportional to the local difference between the dissolution and precipitation rate and is given by, see e.g. [6]

$$\rho_c v_n(c_1, c_2, x) = -(k_p r(c_1, c_2) - k_d w(x)), \tag{2.4}$$

where k_p and k_d are positive rate constants $[\frac{\mathrm{mol}}{\mathrm{m\ s}}]$ and where $r(c_1, c_2)$ is a rate function describing the precipitation rate. A typical example is given by the law of mass action kinetics, leading to

$$r(c_1, c_2) = k_m c_1^{n_1} c_2^{n_2}, \tag{2.5}$$

with k_m $[\left(\frac{\mathrm{mol}}{\mathrm{m}}\right)^{-(n_1+n_2)}]$ a constant. The dissolution rate $w(x)$ is set valued and is given by

$$w(x) \in H(dist(x, \Gamma)),$$

where *dist* denotes the Euclidian distance function, and H denotes the set-valued Heaviside graph,

$$H(u) = \begin{cases} \{0\}, & \text{if} \quad u < 0, \\ [0, 1], & \text{if} \quad u = 0, \\ \{1\}, & \text{if} \quad u > 0. \end{cases}$$

For a more extensive derivation and discussion of the dissolution and precipitation rates, we refer to [6] and [15].

The normal velocity of the interface can be written as

$$v_n = (0, d_t) \cdot \nu. \tag{2.6}$$

Combining (2.3), (2.4), and (2.6), we obtain the following equation for d:

$$\rho_c d_t \in k(r(c_1, c_2) - H(d))\sqrt{1 + (d_x)^2}. \tag{2.7}$$

At the parts of the boundary $\Gamma_i(t)$ and $\Gamma_o(t)$, we impose

$$\begin{cases} c_1 = c_{b1} \quad \text{and} \quad c_2 = c_{b2} & \text{on} \quad \Gamma_i(t), \\ \partial_x c_1 = \partial_x c_2 = 0 & \text{on} \quad \Gamma_o(t), \end{cases}$$

where c_{b1} and c_{b2} are given non-negative constants.

Now we turn to the equations that describe the fluid flow, and to the boundary conditions that couple the flow with the dissolution/precipitation process. The fluid flow is assumed to be described by the Stokes equations

$$\mu \Delta q = \nabla p,$$
$$\nabla \cdot q = 0,$$

for the fluid velocity q $[\frac{\mathrm{m}}{\mathrm{s}}]$ and pressure p $[\frac{\mathrm{kg}}{\mathrm{m\ s^2}}]$, where μ $[\frac{\mathrm{kg}}{\mathrm{m\ s}}]$ denotes the viscosity. In order to derive a boundary condition for q, we need to consider the molar concentration of the fluid phase c_f. By conservation of mass, we obtain the boundary condition

$$\nu \cdot (D\nabla c_f - qc_f) = -v_n c_f \text{ on } \Gamma_g(t), \tag{2.8}$$

Combining (2.2) and (2.8), and using the assumption (2.1), we obtain

$$\nu \cdot q(t) = \frac{\rho_f - (n_1 + n_2)\rho_c}{\rho_f} v_n.$$

Assuming no slip along the boundary, so that the flow is perpendicular to the boundary, gives

$$q = K v_n \nu, \text{ on } \Gamma_g(t),$$

where the constant K is given by

$$K = \frac{\rho_f - (n_1 + n_2)\rho_c}{\rho_f}. \tag{2.9}$$

The boundary condition for q at the parts of the boundary $\Gamma_i(t)$ and $\Gamma_o(t)$ has to be such that it is consistent with $\nabla \cdot q = 0$. Therefore we impose $q = q_b$ on $\Gamma_i(t)$ and $\Gamma_o(t)$, where q_b is given such that

$$\int_{\Gamma_i(t)\cup\Gamma_o(t)} \nu \cdot q = -\int_{\Gamma_g(t)} K v_n.$$

2.1. Dimensionless form. We make the simplifying assumptions $n_1 = n_2$ and $c_1(x, y, 0) = c_2(x, y, 0)$, and look for solutions such that $c_1(x, y, t) = c_2(x, y, t) = c(x, y, t)$. We introduce reference values t_{ref}, $x_{ref} := L$ and $y_{ref} := L$ for the time and space variables t, x and y. We also introduce a reference value for the concentration c, denoted by c_{ref}, a reference value q_{ref} for the fluid velocity given by $q_{ref} := L/t_{ref}$, and a reference value for the pressure denoted by p_{ref}. Defining the dimensionless quantities

$$\begin{aligned}
&t := t/t_{ref}, \quad x := x/x_{ref}, \quad y := y/y_{ref}, \quad \epsilon := l/L, \\
&u^\epsilon := c/c_{ref}, \quad d^\epsilon := d/l, \quad q^\epsilon := q/q_{ref}, \quad p^\epsilon := p/p_{ref}, \quad \rho_f := \rho_f/c_{ref}, \quad u_f := c_f/c_{ref}, \\
&\rho := \frac{n_1\rho_c}{c_{ref}}, \quad r(u) := \frac{k_p}{k_d} r(c_{ref}u), \quad k := \frac{k_d t_{ref}}{\rho_c l}, \quad D := \frac{D t_{ref}}{L^2}, \quad \mu := \frac{\mu L q_{ref}}{l^2 p_{ref}},
\end{aligned}$$

yields the equations

$$\begin{cases}
u^\epsilon_t = \nabla \cdot (D\nabla u^\epsilon - q^\epsilon u^\epsilon), \\
\epsilon^2 \mu \Delta q^\epsilon = \nabla p^\epsilon, \\
\nabla \cdot q^\epsilon = 0, \\
u^\epsilon,\ q^\epsilon \text{ and } p^\epsilon \text{ symmetric around } y = 0,
\end{cases} \quad \text{in } \Omega^\epsilon(t), \tag{2.10}$$

$$\begin{cases}
d^\epsilon_t = k(r(u^\epsilon) - w)\sqrt{1 + (\epsilon d^\epsilon_x)^2}, \\
w \in H(d^\epsilon), \\
\nu^\epsilon \cdot (D\nabla u^\epsilon - q^\epsilon u^\epsilon) = -\epsilon k(r(u^\epsilon) - w)(\rho - u^\epsilon), \\
q^\epsilon = -\epsilon K k(r(u^\epsilon) - w)\nu^\epsilon,
\end{cases} \quad \text{on } \Gamma^\epsilon(t) \tag{2.11}$$

$$\begin{cases}
u^\epsilon(x, y, 0) = u_0(x, y), \\
d^\epsilon(x, 0) = d_0(x).
\end{cases} \tag{2.12}$$

where

$$\Omega^\epsilon(t) := \{(x,y)|0 \le x \le 1,\ -\epsilon(1/2 - d^\epsilon(x,t)) \le y \le \epsilon(1/2 - d^\epsilon(x,t))\}, \quad (2.13)$$
$$\Gamma^\epsilon(t) := \{(x,y)|x = L,\ -\epsilon(1/2l - d^\epsilon(x,t)) \le y \le \epsilon(1/2l - d^\epsilon(x,t))\}, \quad (2.14)$$

and where

$$\nu^\epsilon = (\epsilon\partial_x d^\epsilon, -1)^T/\sqrt{1 + (\epsilon\partial_x d^\epsilon)^2}, \quad (2.15)$$

denotes the normal on the lower boundary. Note that we do not mention the dimensionless boundary conditions on the parts of the boundary $\Gamma_i(t)$ and $\Gamma_o(t)$. These boundary conditions are not essential in the discussion that will follow. However, they should be such that they are consistent with $\nabla \cdot q^\epsilon = 0$.

By the scaling, the restriction that $d < 1/2l$ now becomes $d^\epsilon < 1/2$.

The dimensionless number k is usually referred to as the Damköhler number and expresses the ratio between the diffusion and the reaction time scale. The auxiliary function w acts as the scaled dissolution rate r_d/k_d. When $d^\epsilon > 0$, w attains the value 1, and when $d^\epsilon = 0$, we have $w = r(u^\epsilon)$. With respect to the reaction rate function $r(u)$, we assume

1. $r : \mathbb{R} \to [0, \infty)$ is locally Lipschitz;
2. a unique $u_- \in [0, \rho)$ exists such that $r(u) = 0$ for all $u \le u_-$ and $r(u)$ is strictly increasing if $u > u_-$.
3. a unique $u_s \in (u_-, \rho)$ exists such that $r(u_s) = 1$.

Note that these assumptions are fulfilled in the typical case of the law of mass action kinetics (2.5).

The dimensionless form of assumption (2.1) is

$$u_f + 2u = \rho_f,$$

so that it makes sense to assume also, based on the physical positivity of u_f, that $u_s < \rho_f/2$. Using this assumption, and the expression (2.9), we obtain the following bounds for K, which we will use later on:

$$\frac{u_s - \rho}{u_s} < K < 1. \quad (2.16)$$

Furthermore, we assume the following inequalities

$$0 \le u_0 < \min(\rho, \rho_f/2),$$
$$0 \le d_0 < 1/2.$$

3. Thin strip. In this section we derive using a formal limiting argument, the effective equations in a thin strip. For completeness, and also for comparison reasons, we first shortly consider the case with a fixed geometry [11].

3.1. Fixed geometry. In this section we will shortly consider the equations (2.10)-(2.12), but formulated on a fixed domain. This corresponds to the situation as studied in [13]. In the cited paper it is proven that for $\epsilon \to 0$, the solutions of the equations on a fixed domain converge to solutions of an effective reactive transport equation. Because we have used here a slightly different scaling as in [13], we shall formally derive the effective equation below, also as a rehearsal for the next section.

In the fixed geometry case we start off with the following set of equations

$$\begin{cases} u^\epsilon_t = \nabla \cdot (D\nabla u^\epsilon - q^\epsilon u^\epsilon), \\ \epsilon^2 \mu \Delta q^\epsilon = \nabla p^\epsilon, \\ \nabla \cdot q^\epsilon = 0, \\ u^\epsilon,\ q^\epsilon \text{ and } p^\epsilon \text{ symmetric around } y = 0, \end{cases} \quad \text{in } \Omega^\epsilon, \tag{3.1}$$

$$\begin{cases} d^\epsilon_t = k(r(u^\epsilon) - w), \\ w \in H(d^\epsilon), \\ D\nu \cdot \nabla u^\epsilon = -\epsilon \rho d^\epsilon_t, \\ q^\epsilon = 0, \end{cases} \quad \text{on } \Gamma^\epsilon \tag{3.2}$$

$$\begin{cases} u^\epsilon(x, y, 0) = u_0(x, y), \\ d^\epsilon(x, 0) = d_0(x). \end{cases} \tag{3.3}$$

where

$$\Omega^\epsilon := \{(x, y) | 0 \le x \le 1,\ -\epsilon/2 \le y \le \epsilon/2\},$$

and where ν denotes the outward pointing normal at the boundary.

Since the domain is fixed, we can solve the equations for the flow independent of the other equations, and we assume Poisseuille flow:

$$q^\epsilon(x, y, t) = (q^{\epsilon(1)}(y), 0), \quad \text{with} \quad q^{\epsilon(1)}(y) = Q(1 - (2y)^2/\epsilon^2),$$

where $Q > 0$ is a given constant (see also [13]), and where the constant pressure gradient is given by

$$\nabla p^\epsilon = (\frac{-8Q\mu}{\epsilon^2},\ 0)^T. \tag{3.4}$$

We assume the following asymptotic expansion for u^ϵ and d^ϵ

$$u^\epsilon(x, y, t) = u_0(x, \frac{y}{\epsilon}, t) + \epsilon u_1(x, \frac{y}{\epsilon}, t) + \epsilon^2(...), \tag{3.5}$$

$$d^\epsilon(x, t) = d_0(x, t) + \epsilon d_1(x, t) + \epsilon^2(...), \tag{3.6}$$

Note that the vertical coordinate of the variables u_i is rescaled so that the $u_i(x, z, t)$ are defined on the square domain $\Omega := \{(x, z) | 0 \le x \le 1,\ -1/2 \le z \le 1/2\}$. We introduce the same scaling for the flow velocity $q^{\epsilon(1)}$

$$q^{\epsilon(1)}(y) = q_0(y/\epsilon), \quad \text{with} \quad q_0(z) = Q(1 - (2z)^2),$$

where $q_0(z)$ is defined on the interval $[-1/2, 1/2]$. If we substitute the expansion for u^ϵ in the convection-diffusion equation, we obtain

$$\partial_t u_0 = \partial_x(D\partial_x u_0 - q_0^{(1)} u_0) + \epsilon^{-1}\partial_z(\epsilon^{-1} D\partial_z u_0 - q_0^{(2)} u_0) + \epsilon^{-1}\partial_z(D\partial_z u_1) \tag{3.7}$$

$$+\partial_y(D\partial_y u_2) - \partial_z(q_1^{(2)} u_0 + q_0^{(2)} u_1) + \epsilon(...), \tag{3.8}$$

and for the boundary condition at $z = -1/2$ we obtain

$$-\epsilon^{-1} D\partial_z u_0 + D\partial_z u_1 + \epsilon D\partial_z u_2 = -\epsilon\partial_t d_0 \rho + \epsilon^2(...),$$

Combining the lowest order terms of both equations gives the following set of equations

$$\begin{cases} \partial_{zz} u_0 = 0, & \text{in } \Omega \\ \partial_z u_0 = 0, & \text{at } z = -1/2, \text{ and } z = 1/2. \end{cases}$$

From these equations we conclude that u_0 does not depend on z.

Now we proceed to integrate the convection/diffusion equation for u^ϵ

$$\frac{1}{\epsilon}\int_{-\epsilon/2}^{\epsilon/2} \partial_t u^\epsilon \, dy = \frac{1}{\epsilon}\int_{-\epsilon/2}^{\epsilon/2} \partial_x(D\partial_x u^\epsilon - q^{\epsilon(1)}) + \partial_y(D\partial_y u^\epsilon - q^{\epsilon(2)} u^\epsilon)\, dy.$$

Interchanging derivation and integrals, and integrating, and using the boundary condition, gives

$$\partial_t\Big(\frac{1}{\epsilon}\int_{-\epsilon/2}^{\epsilon/2} u^\epsilon \, dy\Big) + 2\partial_t d^\epsilon \rho = \partial_x\Big(\frac{1}{\epsilon}\int_{-\epsilon/2}^{\epsilon/2} (D\partial_x u^\epsilon - q^{\epsilon(1)} u^\epsilon)\, dy\Big)$$

In deriving the equation above we have so far not used the asymptotic expansions (3.5)-(3.6). Now we will substitute the expansions in the equation above and retain only the terms independent of ϵ

$$\partial_t\Big(\int_{-1/2}^{1/2} u_0(x,z,t)\, dz\Big) + 2\partial_t d_0(x,t)\rho = \partial_x\Big(\int_{-1/2}^{1/2} (D\partial_x u_0(x,z,t) - q_0(z) u_0(x,z,t))\, dz\Big).$$

Subsequently we use that u_0 does not depend on z, i.e., $u_0 = u_0(x,t)$, and obtain

$$\partial_t(u_0 + 2\rho d_0) = \partial_x(D\partial_x u_0 - \bar{q} u_0), \tag{3.9}$$

where $\bar{q}$ denotes the averaged velocity

$$\bar{q} = \int_{-1/2}^{1/2} q_0(z)\, dz = \frac{2}{3} Q.$$

In order to derive an effective equation for d_0, we first regularize the set-valued Heaviside graph, so that we obtain

$$d_t^\epsilon = k(r(u^\epsilon) - H_\delta(d^\epsilon)),$$

where, for $\delta > 0$,

$$H_\delta(d) := \begin{cases} 0 & \text{if } d < 0, \\ d/\delta & \text{if } d \in [0, \delta], \\ 1, & \text{if } d > \delta. \end{cases}$$

Since r and H_δ are both Lipschitz, we now write, after substituting the asymptotic expansions (3.5)-(3.6)

$$\partial_t d_0 = k(r(u_0) - H_\delta(d_0)) + \epsilon(...).$$

Only keeping terms independent of ϵ, and letting $\delta \to 0$, we obtain

$$\partial_t d_0 \in k(r(u_0) - H(d_0)). \tag{3.10}$$

The system of equations formed by (3.9) and (3.10) is, up to a different scaling, precisely the system of equations studied in [11] and in [13] it is proved that this system of equations is also the result of a rigorous argument.

3.2. Variable geometry. In this section we will repeat the formal procedure presented in the previous section, but now for the equations (2.10)-(2.12), which are defined on the variable domain $\Omega^\epsilon(t)$ as given in (2.13). We again assume the asymptotic expansions (3.5) and (3.6) for u^ϵ and d^ϵ, and in addition we asssume the expansions

$$q^\epsilon(x, y, t) = q_0(x, \frac{y}{\epsilon}, t) + \epsilon q_1(x, \frac{y}{\epsilon}, t) + \epsilon^2(...), \tag{3.11}$$

$$p^\epsilon(x, y, t) = p_0(x, \frac{y}{\epsilon}, t) + \epsilon p_1(x, \frac{y}{\epsilon}, t) + \epsilon^2(...), \tag{3.12}$$

for q^ϵ and p^ϵ, since we cannot solve for q^ϵ and p^ϵ independent of the other unknowns anymore. Also note again that the vertical coordinate of the variables $u_i(x, z, t)$, $q_i(x, z, t)$ and $p_i(x, z, t)$ are rescaled so that they are defined on the domain

$$\Omega(t) := \{(x, z) | 0 \le x \le 1,\ -1/2 + d^\epsilon \le z \le 1/2 - d^\epsilon\}.$$

We again substitute the expansion for u^ϵ in the convection-diffusion equation and we obtain, similarly as before, the equation (3.8). For the boundary condition we obtain

$$\epsilon\partial_x d_0(D\partial_x u_0 - q_0^{(1)} u_0) - (\epsilon^{-1} D\partial_y u_0 - q_0^{(2)} u_0) + D\partial_y u_1 + \epsilon D\partial_y u_2 + \epsilon(q_1^{(2)} u_0 + q_0^{(2)} u_1) = \\ -\epsilon\partial_t d_0(\rho - u_0) + \epsilon^2(...),$$

at $z = -(1/2 - d^\epsilon)$. Combining the lowest order terms of both equations gives the following set of equations

$$\begin{cases} \partial_{zz} u_0 = 0, & \text{in } \Omega \\ \partial_z u_0 = 0, & \text{at } z = -1/2 + d^\epsilon, \text{ and } z = 1/2 - d^\epsilon. \end{cases}$$

From these equations we conclude again that u_0 does not depend on z.

Integrating the convection/diffusion equation for u^ϵ gives

$$\frac{1}{\epsilon}\int_{-\epsilon(1/2-d^\epsilon)}^{\epsilon(1/2-d^\epsilon)} \partial_t u^\epsilon \, dy = \frac{1}{\epsilon}\int_{-\epsilon(1/2-d^\epsilon)}^{\epsilon(1/2-d^\epsilon)} \partial_x(D\partial_x u^\epsilon - q^{\epsilon(1)}) + \partial_y(D\partial_y u^\epsilon - q^{\epsilon(2)}u^\epsilon)\, dy.$$

Interchanging derivation and integrals results in

$$\begin{aligned}\partial_t\Big(\frac{1}{\epsilon}\int_{-\epsilon(1/2-d^\epsilon)}^{\epsilon(1/2-d^\epsilon)} u^\epsilon \, dy\Big) + 2\partial_t d^\epsilon u^\epsilon|_{y=-\epsilon(1/2-d^\epsilon)} = \\ \partial_x\Big(\frac{1}{\epsilon}\int_{-\epsilon(1/2-d^\epsilon)}^{\epsilon(1/2-d^\epsilon)} (D\partial_x u^\epsilon - q^{\epsilon(1)}u^\epsilon)\, dy\Big) \\ +2\partial_x d^\epsilon (D\partial_x u^\epsilon - q^{\epsilon(1)}u^\epsilon)|_{y=-\epsilon(1/2-d^\epsilon)} \\ -\frac{2}{\epsilon}(D\partial_y u^\epsilon - q^{\epsilon(2)}u^\epsilon)|_{y=-\epsilon(1/2-d^\epsilon)}\end{aligned}$$

Using the boundary condition (2.11_3), we obtain

$$\begin{aligned}\partial_t\Big(\frac{1}{\epsilon}\int_{-\epsilon(1/2-d^\epsilon)}^{\epsilon(1/2-d^\epsilon)} u^\epsilon \, dy\Big) + 2\partial_t d^\epsilon u^\epsilon|_{y=-\epsilon(1/2-d^\epsilon)} = \\ \partial_x\Big(\frac{1}{\epsilon}\int_{-\epsilon(1/2-d^\epsilon)}^{\epsilon(1/2-d^\epsilon)} (D\partial_x u^\epsilon - q^{\epsilon(1)}u^\epsilon)\, dy\Big) \\ -2\partial_t d^\epsilon(\rho - u^\epsilon)|_{y=-\epsilon(1/2-d^\epsilon)}.\end{aligned} \tag{3.13}$$

Now we substitute the expansions (3.5), (3.6) and (3.11) in the equation (3.13) and retain only the terms independent of ϵ:

$$\begin{aligned}\partial_t\Big(\int_{-(1/2-d_0)}^{(1/2-d_0)} u_0(x,z,t)\, dz\Big) + 2\partial_t d_0(x,t)u_0(x,z,t)|_{z=-(1/2-d_0(x,t))} = \\ \partial_x\Big(\int_{-(1/2-d_0)}^{(1/2-d_0)} (D\partial_x u_0(x,z,t) - q_0^{(1)}(x,z,t)u_0(x,z,t))\, dz\Big) \\ -2\partial_t d_0(x,t)(\rho - u_0(x,z,t))|_{z=(1/2-d_0(x,t))}.\end{aligned}$$

We use that u_0 does not depend on z, i.e., $u_0(x,z,t) = u_0(x,t)$, and obtain

$$\partial_t((1-2d_0)u_0 + 2\rho d_0) = \partial_x(D(1-2d_0)\partial_x u_0 - \bar{q}u_0), \tag{3.14}$$

where $\bar{q}$ denotes the averaged velocity

$$\bar{q} = \int_{-1/2+d_0}^{1/2-d^0} q_0^{(1)}\, dz.$$

Now we turn our attention to the flow problem. We integrate both sides of the equation $\nabla \cdot q^\epsilon = 0$ over a portion of the strip of length δx, denoted by

$$Y = \{(v,w) | x \le v \le x + \delta x, |w| \le \epsilon(1/2 - d)\}.$$

We compute

$$0 = \int_Y \nabla \cdot q \, dV = \int_{-\epsilon(1/2-d)}^{\epsilon(1/2-d)} q^{(1)}|_{x=x_1+\delta x} \, dy - \int_{-\epsilon(1/2-d)}^{\epsilon(1/2-d)} q^{(1)}|_{x=x_1} \, dy + 2\int_{x_1}^{x_1+\delta x} \nu \cdot q|_{y=\epsilon(1/2-d)} \sqrt{1+(\epsilon d_x)^2} \, dx.$$

Dividing by δx, taking the limit $\delta x \to 0$ and collecting lowest order terms in ϵ gives

$$\partial_x \bar{q} - 2K\partial_t d_0 = 0. \tag{3.15}$$

Substituting the expansions for q^ϵ and p^ϵ in $(2.10_{2,3})$ and collecting the terms with the lowest order in ϵ yields the set of equations

$$\begin{aligned} &\partial_z p_0 = 0, \\ &\mu \partial_{zz} q_0^{(1)} = \partial_x p_0, \\ &q_0^{(1)} = q_0^{(2)} = 0 \quad \text{for} \quad z = -1/2 + d_0 \quad \text{and} \quad z = 1/2 - d_0. \\ &\partial_z q_0^{(2)} = 0 \end{aligned}$$

We conclude that p_0 does not depend on the z-coordinate, and that $q_0^{(2)} \equiv 0$. Furthermore, we can solve for $q_0^{(1)}$ in terms of $\partial_x p_0$

$$q_0^{(1)}(x,z,t) = (z^2 - (1/2 - d^0(x,t))^2)\frac{\partial_x p_0(x,t)}{2\mu}.$$

Integrating this equation along the z-coordinate yields

$$\bar{q} = \frac{\partial_x p_0}{2\mu}\int_{-1/2+d_0}^{1/2-d_0} (z^2 - (1/2-d^0)^2)\, dz = -\frac{2\partial_x p_0}{3\mu}(1/2-d_0)^3,$$

so that we can now write an expression for the pressure gradient

$$\partial_x p_0 = -\frac{3\mu\bar{q}}{2(1/2-d_0)^3}.$$

In order to derive an effective equation for d_0, we, as before, first regularize the set-valued Heaviside graph, so that we obtain

$$d_t^\epsilon = k(r(u^\epsilon) - H_\delta(d^\epsilon))\sqrt{1+(\epsilon d_x^\epsilon)^2}.$$

Since r and H_δ are both Lipschitz, we obtain, after substituting the asymptotic expansions (3.5)-(3.6) an only keeping terms independent of ϵ, and letting $\delta \to 0$, again (3.10)

Collecting the equations (3.14), (3.15) and (3.10), we arrive at the following system of equations, for the unknows $u_0(x,t)$, $\bar{q}(x,t)$ and $d_0(x,t)$

$$\begin{cases} \partial_t((1-2d_0)u_0 + 2\rho d_0) = \partial_x(D(1-2d_0)\partial_x u_0 - \bar{q}u_0), \\ \partial_x \bar{q} - 2K\partial_t d_0 = 0, \\ \partial_t d_0 \in k(r(u_0) - H(d_0)). \end{cases}$$

4. Travelling waves. For the system of equations formed by (3.9) and (3.10), which corresponds to the case where the thickness of the crystalline layer attached to the boundary of the strip is assumed to be negligible, travelling wave solutions are studied in [11]. In this section we will study travelling wave solutions of the system we derived in the previous section, where we have taken into account the thickness of the crystalline layer. We will prove the existence and uniqueness of travelling wave solutions, and in the proofs we will follow closely parts of Sections 1, 2 and 3 of [11].

For notational convenience we drop the subscripts and bars form the unknowns, and we study the following system of equations for the unknown functions $u(x,t)$, $d(x,t)$ and $q(x,t)$

$$\begin{cases} \partial_t((1-2d)u+2\rho d) - \nabla\cdot((1-2d)D\nabla u - qu) = 0, \\ \partial_t d \in k(r(u)-H(d)), \\ \partial_x q - 2K\partial_t d = 0. \end{cases} \tag{4.1}$$

We look for non-negative travelling wave solutions, i.e. $u = u(\eta)$, $d = d(\eta)$ and $q = q(\eta)$ with $\eta = x - at$, and $d < 1/2$, satisfying

$$\left.\begin{array}{l} -a((1-2d)u+2\rho d)' - ((1-2d)Du' - qu)' = 0, \\ -ad' \in k(r(u)-H(d)), \\ q' + 2aKd' = 0, \end{array}\right\} \quad \text{in } \mathbb{R}.$$

and boundary conditions

$$\begin{aligned} &u(-\infty) = u^*,\ u(\infty) = u_*, \\ &d(-\infty) = d^*,\ d(\infty) = d_*, \\ &q(-\infty) = q^*, \end{aligned} \tag{4.2}$$

where we assume that $0 \le u^*, u_*, q^*$ and $0 \le d^*, d_* < 1/2$. To define the notion of solutions of the travelling wave equations we introduce

$$w := \frac{1}{k}(ad' + kr(u)) \in H(d),$$

as a new variable.

Definition 4.1. *The set (u,d,w,q,a) with u, d, w and q being functions defined on $\mathbb{R}$ and a a real number, is called a travelling wave if*

(i) $u \in C^1(\mathbb{R})$, $d \in C^1_{pw}(\mathbb{R})$, $w \in C_{pw}(\mathbb{R})$, $q \in C^1_{pw}(\mathbb{R})$,

(ii) $u,\ w \ge 0$, *and* $0 \le d < 1/2$

(iii) $q' + 2aKd' = 0$,

(iv) $0 \le w \le 1$, $w = 1$ *on* $\{d > 0\}$,

(v) $((1-2d)Du' + 2a\rho d)' = (qu - a(1-2d)u)'$,

(vii) $-ad' + kw = kr(u)$,

(viii) u, d and q satisfy the boundary conditions (4.2).

We use $C_{pw}(\mathbb{R})$ to denote the piecewise continuous functions on $\mathbb{R}$ (with finitely many points of discontinuity), which are continuous from the right and $C^1_{pw}(\mathbb{R})$ to denote those $u \in C(\mathbb{R})$ for which $f \in C_{pw}(\mathbb{R})$ exists such that $u' = f$ except at the points of discontinuity of f.

Integrating equation (iii) in Definition 4.1, we obtain

$$q = q^* + 2aK(d^* - d). \tag{4.3}$$

For $\eta \to \infty$, we obtain

$$q_* := q(+\infty) = q^* + 2aK\Delta d,$$

where $\Delta d := d^* - d_*$. Integration of the equation in Definition 4.1(v) leads to

$$(1-2d)Du' + 2a\rho d = qu - a(1-2d)u + A, \tag{4.4}$$

for some $A \in \mathbb{R}$. For $\eta \to \pm\infty$ this equation leads to a set of equations for a and A, which results in

$$a = \frac{\Delta u}{(2\rho + 2Ku_*)\Delta d + \Delta((1-2d)u)} q^*, \tag{4.5}$$

$$A = a(2\rho d^* + (1-2d^*)u^*) - q^* u^*, \tag{4.6}$$

where $\Delta u := u^* - u_*$, $\Delta d := d^* - d_*$ and $\Delta((1-2d)u) := (1-2d^*)u^* - (1-2d_*)u_*$. Substituting (4.6) in (4.4) gives the following equation for u

$$(1-2d)Du' = (q^* - a)(u - u^*) - 2a(\rho + Ku)(d - d^*) + 2a(du - d^*u^*). \tag{4.7}$$

For a travelling wave to exist, we need that the boundary conditions on u and d are equilibrium points for the differential equations. Considering the u-equation this is guaranteed by the expression for the wave speed. For the d-equation, it requires the additional conditions

$$\begin{aligned} 0 &\in k(r(u^*) - H(d^*)) \\ 0 &\in k(r(u_*) - H(d_*)) \end{aligned} \tag{4.8}$$

We first investigate the possible combinations of boundary conditions for which travelling waves can exist:

- $d_*, d^* > 0$ and $d_* \neq d^*$: then it follows from (4.8) that $u^* = u_* = u_s$. By (2.16), the denominator in (4.5) is not equal zero, and we have $a = 0$. In this case (4.7) implies that $u = u_s$ on $\mathbb{R}$. This solution describe the situation of an abitrary, stationary crystal distribution in the presence of saturated fluid.

- $d_* = d^* = 0$ and $u^* \neq u_*$: in this case $a = q^*$ and (4.7) reduces to

  $$(1-2d)u' = -2q^* d(\rho - u)$$

  Now we need to consider two cases: a) $d = 0$ on $\mathbb{R}$. This implies $u = u_s$ which is in contradiction with the boundary conditions. b) $d(\eta_0) > 0$ and $d'(\eta_0) = 0$ for some η_0. This implies $u(\eta_0) = u_s$ and $u(\eta) > u_s$ for $\eta < \eta_0$. This means that $u^* > u_s$, which is in contradiction with the boundary condition (4.8_1).

Thus to obtain a non-trivial solution we need that precisely one of the boundary conditions on d is zero. We are left with the following two classes

$$I \begin{cases} d_* > 0, & d^* = 0 \\ u_* = u_s, & 0 \leq u^* < u_s \end{cases}$$
$$II \begin{cases} d^* > 0, & d_* = 0 \\ u^* = u_s, & 0 \leq u_* < u_s \end{cases}$$

It can easily be checked, using the bounds (2.16), that for both classes $q^* > a > 0$.

We do not consider the cases

$$d^* = d_* > 0, \quad u^* = u_* = u_s, \quad \text{and}$$
$$d^* = d_* = 0, \quad u^* = u_* \leq u_s.$$

In these cases the wave speed a is not uniquely determined. For arbitrary a there exist the trivial constant solutions. Just as in [11] we do not think that there exist non-trivial solutions in these cases, but we cannot exclude these at the moment.

We state the following proposition without proof, as the proof runs exactly along the lines of the proof of Proposition 2.1 in [11].

PROPOSITION 4.2. *Let (u, d, w, q, a) be a travelling wave with boundary conditions from class I or class II. Then*

(i) $u < u_s$ on $\mathbb{R}$,

(ii) d is continuously differentiable and $d' > 0$ in $\{d > 0\}$.

The second statement in Proposition 4.2 immediately gives:

COROLLARY 4.3. *No travelling wave exists with boundary conditions from class II.*

The following proposition is part (i) of Proposition 2.3 in [11], to which paper we refer to for the proof.

PROPOSITION 4.4. *There exists an $L \in \mathbb{R}$ such that*

$$d(\eta) = \begin{cases} 0 & \text{for } -\infty < \eta \leq L, \\ > 0 & \text{for } \eta > L. \end{cases}$$

Now we are in a position to proof the following existence result.

THEOREM 4.5. *For any set of boundary conditions from class I, there exists a travelling wave.*

Proof. We set the L from Proposition 4.4 by translation to $L = 0$, which means that the solution has to satisfy

$$d(\eta) > 0 \text{ for } \eta > 0,$$
$$d(\eta) = 0 \text{ for } \eta \leq 0,$$
$$w(\eta) = 1 \text{ for } \eta > 0.$$

The travelling wave functions u, d and w are found by matching the solutions of the following initial value problems:

$$(P^+)\begin{cases} u' = \frac{(q^*-a)(u-u^*)-2ad(\rho-(1-K)u)}{(1-2d)D} =: f_1(u,d) & \text{for } \eta > 0, \\ d' = \frac{k}{a}(1-r(u)) =: f_2(u,d) & \text{for } \eta > 0, \\ u(0) = u_0 \in (u^*, u_s), \text{ and } d(0) = 0. \end{cases}$$

$$(P_-)\begin{cases} u' = \frac{q^*-a}{D}(u-u^*) & \text{for } \eta < 0, \\ w = r(u) & \text{for } \eta < 0, \\ u(0) = u_0. \end{cases}$$

We will now use a shooting argument in the u, d phase plane. First we will proof the existence of an initial value u_0 for Problem (P^+) such that

$$(u(\eta), d(\eta)) \to (u_s, d_*) \text{ as } \eta \to \infty.$$

Subsequently we solve for this value of u_0 Problem (P^-).

We investigate the sign of the functions f_1 and f_2. We have for $u^* \in [u^*, u_s]$, $d \in [0, d_*]$:

$$f_1(u,d) > 0 \,(\text{resp. } < 0) \Leftrightarrow f(u) := \frac{(q^*-a)(u-u^*)}{2a(\rho-(1-K)u)} < d \,(\text{resp. } > d),$$
$$f_2(u,d) > 0 \Leftrightarrow u < u_s.$$

It is clear that $f(u)$ is increasing for $u > 0$. Further more, we have $f(u^*) = 0$, and, by the expression (4.5) for a, we have $f(u_s) = d_*$.

For the set $S := \{(u,d) | u^* < u < u_s,\, d_* < d < f(u)\}$ we consider the following parts of its boundary

$$\partial S_1 := \{(u,d) | u^* < u < u_s,\, d = f(u)\},$$
$$\partial S_2 := \{(u,d) | u = u_s,\, 0 < d < d_*\}.$$

In the interval (u^*, u_s) we distinguish the subsets A and B according to the following criteria. We say that $\alpha \in A$ if the positive half-orbit corresponding to the solution of Problem (P^+) with $u(0) = \alpha$, $d(0) = 0$ leaves the set S through the boundary ∂S_1. Similarly, $\beta \in B$ if the positive half-orbit staring from $u(0) = \beta$, $d(0) = 0$ leaves the set S through ∂S_2. Proceeding as in [10, 11], one shows that the sets A and B are non-empty, open and ordered. Hence $\sup A =: \bar{\alpha} \le \bar{\beta} := \inf B$, where $\bar{\alpha} \notin A$ and $\bar{\beta} \notin B$.

This means that for any $u_0 \in [\bar{\alpha}, \bar{\beta}]$ the half-orbit corresponding to Problem (P^+) ends up in the point (u_s, d_*) as $\eta \to \infty$. This gives the required solution in terms of $u = u(\eta)$, $d = d(\eta)$ for $\eta > 0$. The solution for $\eta < 0$ is obtained by explicitly solving (P^-):

$$u(\eta) = (u_0 - u^*) \exp\left(\frac{q^*-a}{D}\eta\right) + u^*. \tag{4.9}$$

It is now easily checked that all the conditions in Definition 4.1 are satisfied. □

THEOREM 4.6. *Suppose there exist two travelling wave solutions, characterized by* (u_1, d_1, w_1, q_1) *and* (u_2, d_2, w_2, q_2)*, for the same boundary conditions from class I. Then there exists* $\eta_0 \in \mathbb{R}$ *such that*

$$(u_1(\cdot), d_1(\cdot), w_1(\cdot), q_1(\cdot)) = (u_2(\cdot + \eta_0), d_2(\cdot + \eta_0), w_2(\cdot + \eta_0), q_2(\cdot + \eta_0)).$$

Proof. Given both travelling waves, we apply to each a shift such that

$$d_1(\eta),\, d_2(\eta) > 0 \quad \text{for} \quad \eta > 0,$$
$$d_1(\eta) = d_2(\eta) = 0 \quad \text{for} \quad \eta \leq 0.$$

Then

$$w_1(\eta) = w_2(\eta) = 1 \quad \text{for} \quad \eta > 0.$$

We assume, without loss of generality, that $u_1(0) > u_2(0)$. Suppose that $u_1(\eta) \leq u_2(\eta)$ for $\eta > 0$, then

$$\lim_{\eta\to\infty} d_1(\eta) = \lim_{\eta\to\infty} \int_0^\eta \frac{k}{a}(1 - r(u_1(\theta))d\theta < \lim_{\eta\to\infty} \int_0^\eta \frac{k}{a}(1 - r(u_2)(\theta)d\theta = \lim_{\eta\to\infty} d_2(\eta),$$

which contradicts the boundary conditions for $\eta \to \infty$. This means that there exists an $\eta^* \in \mathbb{R}$, with $\eta^* > 0$, such that $u_1(\eta^*) < u_2(\eta^*)$, and by the continuous differentiability of u_1 and u_2, there exists an $\eta_* \in \mathbb{R}$, with $\eta_* > 0$, such that

$$u_1(\eta_*) = u_2(\eta_*), \tag{4.10}$$
$$u_1(\eta) \geq u_2(\eta) \quad \text{for} \quad \eta \in [0, \eta_*], \tag{4.11}$$
$$u_1'(\eta_*) \leq u_2'(\eta_*). \tag{4.12}$$

By (4.11), it holds that $d_1(\eta_*) < d_2(\eta_*)$. We compute, using (4.7) and (4.10),

$$u_1'(\eta_*) - u_2'(\eta_*) = 2\frac{[(q^* - a)(u_1(\eta_*) - u^*) - a(\rho - Mu_1(\eta_*))](d_1(\eta_*) - d_2(\eta_*))}{(1 - 2d_1(\eta_*))(1 - 2d_2(\eta_*))D}, \tag{4.13}$$

where $M = 1 - K$. It is now our aim to derive a contradiction to (4.12), so let us focus on the sign of

$$(q^* - a)(u_1(\eta_*) - u^*) - a(\rho - Mu_1(\eta_*)).$$

Using the expression (4.5) for the wave speed a, we obtain

$$(q^* - a)(u_1(\eta_*) - u^*) - a(\rho - Mu_1(\eta_*)) =$$
$$q^*\frac{-(u_s - u^*)(\rho + Ku_1(\eta_*) - u^*) + (u_1(\eta_*) - u^*)[2d_*(\rho - u_sM) + u_s - u^*]}{2d_*(\rho - u_s(1 - K)) + u_s - u^*}.$$

Now, using $d_* < 1/2$, $u^* < u_s$, $u < u_s$ and the bounds (2.16) on K, we estimate

$$(q^* - a)(u_1(\eta_*) - u^*) - a(\rho - Mu_1(\eta_*)) <$$
$$q^*\frac{-(u_s - u^*)(\rho + Ku_1(\eta_*) - u^*) + (u_1(\eta_*) - u^*)[(\rho - u_sM) + u_s - u^*]}{2d_*(\rho - u_sM) + u_s - u^*}$$
$$= \frac{q^*(u_1(\eta_*) - u_s)(\rho - Mu^*)}{2d_*(\rho - u_sM) + u_s - u^*} < 0.$$

Together with (4.13), this gives $u_1'(\eta_*) - u_2'(\eta_*) > 0$, which contradicts (4.12). This means that our original assumption that $u_1(0) > u_2(0)$ (and thus also the assumption $u_1(0) < u_2(0)$) does not hold, so that we have $u_1(0) = u_2(0)$, which implies that $u_1 = u_2$, $d_1 = d_2$, $w_1 = w_2$ and $q_1 = q_2$ on $\mathbb{R}$. □

5. Fixed vs. variable geometry. In this section we compare the travelling wave solutions of the fixed geometry case as studied in [11] and the travelling wave solutions of the variable geometry case as studied in the previous sections. In particular, we are interested in comparing the wave speeds for both situations. In order to do so, we introduce a parameter α and formulate the system of equations

$$\begin{cases} \partial_t((1-2\alpha d)u + 2\rho d) - \nabla \cdot ((1-2\alpha d)\nabla u - qu) = 0, \\ \partial_t d \in k(r(u) - H(d)), \\ \partial_x q - 2\alpha K \partial_t d = 0. \end{cases} \tag{5.1}$$

For $\alpha = 1$, we are in the case we have discussed in the previous section, and for $\alpha = 0$ we are in the case as discussed in [11]. It can be checked that all the results presented in the previous section also hold true for all $\alpha \in [0, 1]$. This means that there exists, for boundary conditions from class I, a unique travelling wave solutions to the system of equations (5.1). The wave speed is then given by

$$a(\alpha) = \frac{u_s - u^*}{2d_*(\rho - \alpha u_s(1-K)) + u_s - u^*} q^*. \tag{5.2}$$

We prove the following proposition.

PROPOSITION 5.1. *For $1 - \rho/u_s < K < 1$ and $0 \le \alpha \le 1$, $a(\alpha)$ is increasing in α*

Proof. Computing the derivative of (5.2) with respect to α, we obtain

$$a'(\alpha) = \frac{u_s - u^*}{(2d_*(\rho - \alpha u_s(1-K)) + u_s - u^*)^2} 2d_* u_s (1-K) q^*.$$

Since for the denominater we have, using the bounds (2.16)

$$2d_*(\rho - \alpha u_s(1-K)) + u_s - u^* \ge 2d_*(\rho - u_s(1-K)) + u_s - u^* \ge u_s - u^* > 0,$$

the proof is complete. □

From the lemma above, we can deduce that dissolution fronts will travel faster in the variable geometry case. This is also confirmed in the numerical experiments in Section 6. Note, however, that we compare the two situations where the inflow velocity is given. This means that in the variable geometry case the pressure drop is larger since part of the flow channel is narrower.

We may also compare the two situations with a given average pressure gradient. We define the average pressure gradient P as follows

$$P := \lim_{\eta \to \infty} \frac{p_0(\eta) - p_0(-\eta)}{2\eta}.$$

For the fixed geometry case, we have according to (3.4) and (3.10)

$$\frac{p_0(\eta) - p_0(-\eta)}{2\eta} = \frac{1}{2\eta} \int_{-\eta}^{\eta} \partial_x p_0(x)\, dx = -\frac{24\eta\mu\bar{q}}{2\eta} = -12\mu q^*,$$

so that $P_{fix} = -12\mu q^*$.

For the variable geometry case, we have

$$\frac{p_0(\eta) - p_0(-\eta)}{2\eta} = \int_{-\eta}^{\eta} \partial_x p_0(x)\, dx = \int_{-\eta}^{\eta} \frac{-3\mu\bar{q}}{2(1/2 - d_0)^3}\, dx = \int_{-\eta}^{\eta} \frac{-3\mu(q^* - 2aKd_0)}{2(1/2 - d_0)^3}\, dx$$

It can be shown that

$$P_{var} = \frac{1}{2} q^* \left(-12\mu - \frac{3\mu(1 - 2\bar{a}Kd_*)}{2(1/2 - d_*)^3} \right),$$

where $\bar{a} = a/q^*$. As the quotient $(1 - 2\bar{a}Kd)/(1/2 - d)^3$ is increasing in d, it follows that $P_{var} < P_{fix}$ for given q^*. Now, however, we fix P simultaneously for both situations, and solve for q^*_{fix} and q^*_{var}:

$$q^*_{fix} = -\frac{P}{12\mu},$$

and

$$q^*_{var} = P \left(-6\mu - \frac{3\mu(1 - 2\bar{a}Kd_*)}{4(1/2 - d_*)^3} \right)^{-1}.$$

For the corresponding wave speeds, we obtain

$$a_{fix} = -\frac{P}{12\mu} \frac{u_s - u^*}{2d_*\rho + u_s - u^*},$$

and

$$a_{var} = P \left(-6\mu - \frac{3\mu(1 - 2\bar{a}Kd_*)}{4(1/2 - d_*)^3} \right)^{-1} \frac{u_s - u^*}{2d_*(\rho - u_s(1 - K)) + u_s - u^*}$$

Equating the two wave speeds, we can solve for u^* in term of d_*:

$$u^* = u_s + \frac{2d_* u_s (1 - K)(1 + (1 - 2d_*)^3 + 2d_*\rho((1 - 2d_*)^3 - 1)}{(1 - 2d_*)^3 - (1 - 2Kd_*)} =: g(d^*).$$

Define the set

$$X := \{(d_*, u^*) | 0 \le u^* < \min(u_s, g(d_*)),\ 0 < d_* < 1/2\}.$$

Then we have that $a_{fix} > a_{var}$ if $(d_*, u^*) \in X$, $a_{fix} = a_{var}$ if $u^* = g(d_*)$ and $a_{fix} < a_{var}$ otherwise.

6. Numerical experiments. In this section we present the results of some numerical experiments, and compare these results with the results obtained in the previous sections. First we will shorlty discuss the numerical methods used for the computations.

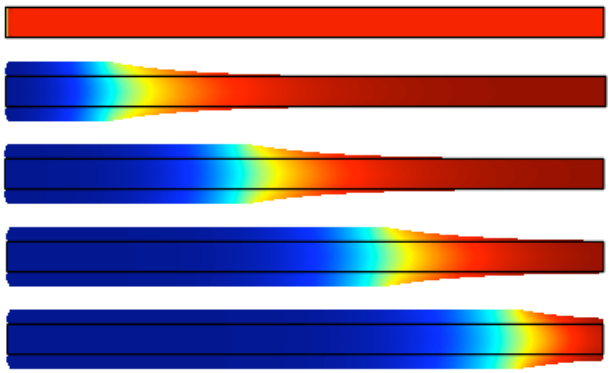

FIG. 6.1. *Concentration profiles of u^ϵ with $\epsilon = 0.1$ for the 2-D model for $t = 0$, $t = 10$, $t = 20$, $t = 30$ and $t = 40$, respectively. Also the changes in the width of the strip are depicted.*

6.1. Arbitrary Lagrangian Eulerian method. For the computation for the microscale model equations we use the arbitrary Lagrangian Eulerian (ALE) method [2]. This method has been developed to solve partial differential equations on moving domains. In this method the partial time derivatives are expressed with respect to a fixed reference configuration. A map, called the ALE map, $\chi_t : \Omega_0 \to \Omega(t)$, associates, at each time t, a point in the current computational domain $\Omega(t)$ to a point in the reference domain Ω_0. In this way, the system of ordinary differential equations resulting after space discretization describes the evolution of the solutions along trajectories that are at all times contained in the computational domain. We use the ALE method as implemented in the COMSOL Multiphysics package [1], with Laplacian smoothing [2]. For more details on the ALE method we refer to [2] and [1].

6.2. Numerical results. In this section we compare the numerical solution of the system (2.10)-(2.12) with that of (4.1) and with that (3.9) and (3.10). The parameter values used for the numerical experiments are

$$\begin{aligned} &D = 10^{-3}, \;\; \rho = 2, \;\; d(x,0) \equiv 0.25, \;\; u(x,0) \equiv 1 = u_s, \\ &u(0,t) = 0, \;\; u_x(L,t) = 0, \;\; k = 0.1, \;\; r(u) = u, \;\; K = 0.1, \\ &q^* = 1/3 \cdot 10^{-1}. \end{aligned}$$

The inflow velocity for the system (2.10)-(2.12), i.e., q^ϵ at $x = 0$, is given by a parabolic velocity profile such that the average velocity matches q^* as given above. At $x = 1$ we impose $p^\epsilon I + \frac{\mu}{2}(\nabla q^\epsilon + (\nabla q^\epsilon)^T) = 0$.

With the parameter values given above we can compute an approximation of the speed of the dissolution front, using (4.5) for the speed of a travelling wave:

$$\begin{aligned} a_{fix} &= \frac{1}{2} q^* = \frac{1}{60} \approx 0.01667, \\ a_{var} &= \frac{20}{31} q^* = \frac{20}{930} \approx 0.02151. \end{aligned}$$

In Fig. 6.1, the concentration profiles of u^ϵ, solving the equations (2.10)-(2.12), are plotted for different values of t. Also the changes in the width of the strip are depicted. These

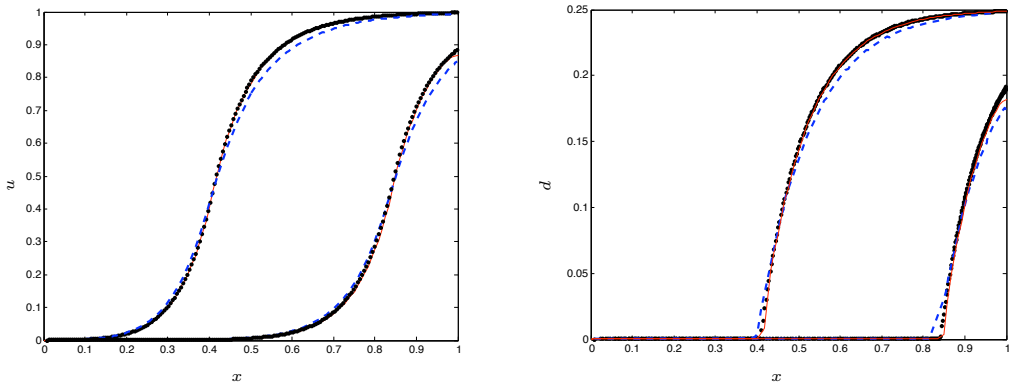

FIG. 6.2. *Profiles of both the 2-D and effective model, for* $t = 20$ *and* $t = 40$. *The left plot shows profiles for* u *and* u^ϵ, *the right plot shows* d *and* d^ϵ. *The thin line represents the solution to the effective model and the dashed line the 2-D model with* $\epsilon = 0.1$ *and the dots represent the 2-D model with* $\epsilon = 0.01$.

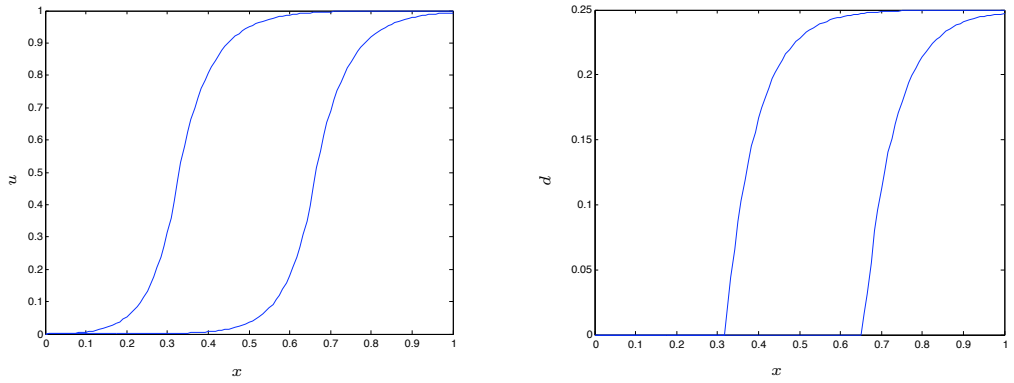

FIG. 6.3. *Profiles of solutions to the effective model for the fixed geometry case, for* $t = 20$ *and* $t = 40$. *The left plot shows profiles for* u, *the right plot shows* d.

profiles are compared to profiles obtained by solving the effective model equations (4.1), in Fig. 6.2. In the left plot the profiles of $u^\epsilon(x, 0, t)$ for two different values of ϵ are compared to the profiles u solving (4.1). In the right plot the d^ϵ is compared to d. The profiles are plotted for the two values $t = 20$ and $t = 40$. The thin continuous lines correspond to u and d, the dashed line corresponds to u^ϵ and d^ϵ for $\epsilon = 0.1$, and the dots correspond to u^ϵ and d^ϵ for $\epsilon = 0.01$. We see that for both values of ϵ the effective model describes the behaviour of solutions of the microscale model quite well, and for $\epsilon = 0.01$ the differences are even hardly distinguishable.

In Fig. 6.3, the profiles of u and d that solve the equations (3.9) and (3.10), corresponding to the fixed geometry case. We see clearly that the front did not move as fast to the right as for the variable geometry case.

In Fig. 6.4, the speed of the dissolution front is showed in more detail. The position of the free boundary of the thickness of the crystalline solid is compared with the wave speed as predicted in (4.5), both for the variable and the fixed geometry case. We see that after a start up phase the speed of the free boundaries matche very well with the predicted values.

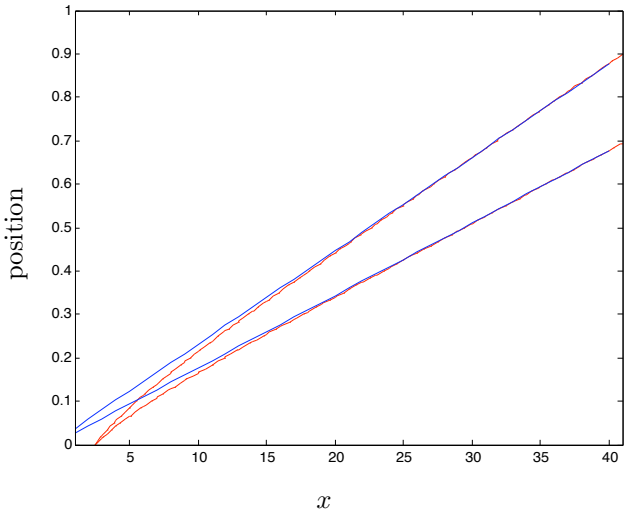

FIG. 6.4. *The position of the free boundary versus time for both the fixed and variable geometry effective models. Two lines with slopes* $a_{fix} = \frac{1}{60} \approx 0.01667$ *and* $a_{var} = \frac{20}{930} \approx 0.02151$ *are also plotted to indicate the wavespeed as predicted in* (4.5).

7. Conclusions. In this paper we have derived a macroscopic model for crystal dissolution and precipitation in porous media. The model takes into account the change in porosity and permeability due to the change in the local pore geometry. The macroscopic model was derived using a formal limiting argument and the behaviour of solutions was validated using numerical experiments.

Also travelling wave solutions of the macroscopic model were studied and compared to travelling wave solutions of previously published models [13, 11]. Just as for the model in [11], only dissolution wave exist. The wave speed for a fixed inflow velocity is faster for the model equations presented in this paper.

Acknowledgements. The author wishes to thank I.S. Pop and C.J. van Duijn for the discussions that helped to shape this work.

REFERENCES

[1] COMSOL Inc. http://www.comsol.com.

[2] J. Donea, A. Huerta, J.-Ph. Ponthot, and A. Rodríguez-Ferran, *Arbitrary Lagrangian–Eulerian methods*, in Encyclopedia of Computational Mechanics, Volume 1: Fundamentals, Chap. 14, E. Stein, R. De Borst, and T. J. R. Hughes, eds., John Wiley & Sons, Ltd., 2004.

[3] R. Eymard, T. Gallouët, R. Herbin, D. Hilhorst, and M. Mainguy, *Instantaneous and noninstantaneous dissolution: approximation by the finite volume method*, in Actes du 30ème Congrès d'Analyse Numérique: CANum '98 (Arles, 1998), vol. 6 of ESAIM Proc., Soc. Math. Appl. Indust., Paris, 1999, pp. 41–55 (electronic).

[4] B. Faugeras, J. Pousin, and F. Fontvieille, *An efficient numerical scheme for precise time integration of a diffusion-dissolution/precipitation chemical system*, Math. Comp., 75 (2006), pp. 209–222 (electronic).

[5] U. Hornung, W. Jäger, and A. Mikelić, *Reactive transport through an array of cells with semi-permeable membranes*, RAIRO Modél. Math. Anal. Numér., 28 (1994), pp. 59–94.

[6] P. Knabner, C. J. van Duijn, and S. Hengst, *An analysis of crystal dissolution fronts in flows though porous media. Part 1: Compatible boundary conditions*, Adv. Water Res., 18 (1995), pp. 171–185.

[7] E. Maisse and J. Pousin, *Diffusion and dissolution/precipitation in an open porous reactive medium*, J. Comput. Appl. Math., 82 (1997), pp. 279–290. 7th ICCAM 96 Congress (Leuven).

[8] A. Tartakovsky, T. Scheibe, G. Redden, P. Meakin, and Y. Fang, *Smoothed particle hydrodynamics model for reactive transport and mineral precipitation*, in Proceedings of the XVI International Conference on Computational Methods in Water Resources, Copenhagen, Denmark, June, 2006. http://proceedings.cmwr-xvi.org, P. J. Binning, P. K. Engesgaard, H. K. Dahle, G. F. Pinder, and W. G. Gray, eds.

[9] A. M. Tartakovsky, P. Meakin, T. D. Scheibe, and R. M. Eichler West, *Simulations of reactive transport and precipitation with smoothed particle hydrodynamics*, J. Comput. Phys., 222 (2007), pp. 654–672.

[10] C. J. van Duijn and P. Knabner, *Solute transport in porous media with equilibrium and nonequilibrium multiple-site adsorption: travelling waves*, J. Reine Angew. Math., 415 (1991), pp. 1–49.

[11] C. J. van Duijn and P. Knabner, *Travelling wave behaviour of crystal dissolution in porous media flow*, European J. Appl. Math., 8 (1997), pp. 49–72.

[12] C. J. van Duijn, L. A. Peletier, and R. J. Schotting, *On the analysis of brine transport in porous media*, European J. Appl. Math., 4 (1993), pp. 271–302.

[13] C. J. van Duijn and I. S. Pop, *Crystal dissolution and precipitation in porous media: pore scale analysis*, J. reine angew. Math., 577 (2004), pp. 171–211.

[14] C. J. van Duijn and R. J. Schotting, *Brine transport in porous media: on the use of von Mises and similarity transformations*, Comput. Geosci., 2 (1998), pp. 125–149.

[15] T. L. van Noorden and I. S. Pop, *A stefan problem modelling dissolution and precipitation in porous media*, tech. report, CASA report 30, Eindhoven University of Technology, 2006.

[16] T. L. van Noorden, I. S. Pop, and M. Röger, *Crystal dissolution and precipitation in porous media: L^1-contraction and uniqueness*, tech. report, CASA report 32, Eindhoven University of Technology, 2006.